Lattice Resistance to Dislocation Motion : A Revisit

A. Dutta[†], M. Bhattacharya[‡], P. Mukherjee[‡], N. Gayathri[‡], G. C. Das[†], and P. Barat[‡*]

[†]*School of Materials Science and Nanotechnology,*

Jadavpur University, Kolkata 700 032, India

[‡]*Variable Energy Cyclotron Centre, 1/AF,*

Bidhannagar, Kolkata 700 064, India

(Dated: January 13, 2019)

Abstract

We present a novel idea to explain the origin of the lattice resistance by modeling a moving dislocation as the dynamic distribution of singularity of the associated elastic field. Numerical implementation of this model shows the existence of a finite potential barrier to dislocation motion arising out of a significant contribution of the linear elastic region surrounding the core and its dependence on the elastic constants of solids. Molecular dynamics simulations are performed and found to produce results in advocacy of the conceptual basis of our model.

PACS numbers: 61.72.Lk, 62.25.-g

Dynamics of dislocations have been studied for decades owing to their fundamental importance in explaining the mechanical behavior of crystalline solids in the plastic regime. A dislocation can move under the influence of a shear load, thereby causing the plastic strains in crystal. However, its motion suffers from the drag forces, pinning and the lattice resistance. The continuum theory of elasticity has been successful in explaining the behavior of dislocations at large length scales. However, the phenomenon of the lattice resistance to dislocation motion demands treatment at the atomistic length scales where the continuum theory of elasticity is believed to be inappropriate. The repeatative discrete atomistic construction of a crystalline solid causes its energy to oscillate periodically with the translation of a gliding dislocation with its Burgers vector as the period of this oscillation. This creates an energy barrier, formally referred to as the Peierls barrier at absolute zero temperature against the motion of the dislocation. The celebrated Peierls-Nabarro (PN) model [1, 2] was the first fruitful analytical attempt to tackle this concept using a hybrid continuum-discrete approach. Nevertheless, it relied upon a multitude of *a priori* assumptions and oversimplifications, which has attracted many critical reviews and modifications till date [3, 4, 5, 6, 7].

In the original PN model, only the misfit between the two half lattices was emphasized and the linear elastic region away from the dislocation core was assumed not to contribute to the lattice resistance [1, 2]. This idea remained unquestioned in all the subsequent modifications of the model and the origin of the lattice resistance is still believed to be the dynamic rearrangment of the bonds at the dislocation core [8]. However, our previous work [9] suggests that the linear elastic region around the dislocation core decisively supplements the core region to cause the overall lattice resistance. This was also conclusively verified with the molecular dynamics (MD) simulations by the demonstration of a change in the dislocation velocity with both the variation of the thickness and the proximity of the dislocation line to the free surface of a thin film. This was attributed to the variation of the lattice resistance and we refer to it as the size effect in the present work. A simplified model in this regard, established the contribution of an atom in the crystal to the overall lattice resistance depending on its position relative to the dislocation line [9]. However, there is still a quest for revealing the origin of this contribution as the existing theories of lattice resistance are found to be inadequate to explain the observed phenomena fully, which compelled us to revisit the fundamental concept of the lattice resistance from a novel standpoint.

In this Letter, we demonstrate the feasibility of introducing the lattice resistance by modeling a moving dislocation as a distributed singularity of the associated elastic field. On implementing this concept numerically to investigate the role of the linear elastic region in determining the lattice resistance, the qualitative features of the results are found to be dependent on the elastic constants of the solids. Similar features are also shown by the MD simulations.

The presence of a dislocation in the solid can be described as a strain field with its singularity at the dislocation line. Any arbitrary displacement in the position of the dislocation line brings the system to an energetically equivalent configuration because of the continuous structure of the solid. Thus, the existence of any potential barrier against the movement of a dislocation line is ruled out. However, we show here that by distinguishing between the descriptions of a moving dislocation in the continuous and discrete structure of the solid, it is possible to incorporate the effect of the lattice resistance. The dislocation line can be considered as a tag for specifying the position of the dislocation in the solid. In crystals with discrete and periodic assembly of atoms, the idea of specifying the position of a dislocation bears a sense only at its equilibrated static sites separated by the length of the Burgers vector. The exact position of the dislocation is inexpressible when the dislocation is moving from an equilibrium site to the next one, as the motion is continuous instead of hopping. It is justifiable to think of a moving dislocation as delocalized and spread out while it is present in between two adjacent static sites. This suggests that the singularity of its strain field may also be distributed simultaneously and this delocalization can directly influence the strain field in the solid. The idea of singularity distribution has long been applied to various fields of physics [10, 11, 12]. The robustness of this approach lies in the fact that it uses the well behaved solutions of the undistributed singularity, in conjunction with the principle of superposition. Thus, in the case of dislocation motion, the line singularity of the associated strain field must be distributed dynamically in such a manner that it becomes again a line singularity after a specific interval of time, when it has shifted from previous line position by the Burgers vector.

A perfect crystal free of defects is in the global minimum of potential energy. A defect like a point defect or dislocation etc., acts as the internal source of strain field. This raises the potential energy density by $\frac{1}{2}C_{ijkl}(\epsilon)\epsilon_{ij}(\mathbf{r},C)\epsilon_{kl}(\mathbf{r},C)$, where C is the stiffness tensor and ϵ is the strain tensor. The interdependence of C and ϵ accounts for the possible non-hookean

behavior observed in the near field of the defect site. The idea of the dynamic change in the singularity distribution of the strain field of a dislocation leads us to expect a perturbation in the field itself. Such a perturbation would change the associated potential energy and if it occurs periodically, as in this case, the system would have to cross over the potential energy barriers periodically for translation of the dislocation. The energy of a moving dislocation, per unit length of the dislocation line, can be expressed as,

$$U(t) = \frac{1}{2} \iint_{\Omega} C_{ijkl}(\epsilon)\epsilon_{ij}(\mathbf{r}, C, t)\epsilon_{kl}(\mathbf{r}, C, t)\, dx\, dy, \tag{1}$$

where Ω is the domain of integration. For a particular operating condition of applied stress and temperature, let ϵ^0 be the strain field at the local minimum of the potential energy and ϵ^b be the change in the strain field at the peak of the potential energy barrier due to the distribution of singularity of the strain field. The contribution of the linear elastic region to the rise in the potential energy and hence to the overall lattice resistance amounts to

$$U_b^l = \frac{1}{2} C_{ijkl} \left[\iint_{\Omega} \left\{ \epsilon_{ij}^0(\mathbf{r})\epsilon_{kl}^b(\mathbf{r}) + \epsilon_{kl}^0(\mathbf{r})\epsilon_{ij}^b(\mathbf{r}) + \epsilon_{kl}^b(\mathbf{r})\epsilon_{ij}^b(\mathbf{r}) \right\} dx\, dy \right]', \tag{2}$$

where the prime indicates that the nonlinear core region is excluded from the integration domain. A finite value of U_b^l justifies the possibility of a significant far field contribution to the overall lattice resistance as exhibited by the size effect [9].

Equations (1) and (2) are used to determine the potential energy as well as its variation due to the distribution of the strain field singularity of an edge dislocation in an isotropic solid, with two independent elastic constants. The calculations are performed for a finite rectangular domain Ω, with an edge dislocation at its origin O as shown in Fig. 1. The domain is divided into small square subdomains with the length of the Burgers vector (b) as its side. We assume a simple homogeneous distribution of the singularity of the strain field of the edge dislocation over the span of one Burgers vector divided into 50 equal divisions as shown in Fig. 2. Consequently, as the dislocation proceeds by one Burgers vector, 99 discrete steps of singularity distribution are required. At each step of the distribution, the magnitude of the Burgers vector per unit length is normalized in such a way, that the total Burgers vector is conserved, as depicted in Fig. 2. The subdomains within a radius $r_c = 2b$ from the dislocation line are excluded from the calculation to avoid the non-linearity of the core. At any particular step of the sigularity distribution, the strain in a subdomain is evaluated by superposing the strains contributed by each of the 50 discrete divisions of the

Burgers vector. The potential energy of each subdomain is calculated using the expressions of the strain field for the edge dislocation [3] and added up to obtain the total potential energy of the whole domain. We alter the dimension of Ω along the y direction to change its thickness and the contribution of linear region to the total potential energy is computed.

Figure 3(a) shows the domain energy at different steps of distribution (in the form of vertical line segments consisting of discrete points) with the variation in the domain thickness keeping the Young's modulus E=1 and the Poisson's ratio ν=0.33. The inset elaborates one such line segment by showing the domain energy at different steps of distribution for a particular thickness of Ω. The rise in the potential energy, when the dislocation is delocalized and away from its static site is obviously more appropriate physically than the relation obtained by the PN model, which assigns a reduced potential energy to the dislocation as it slightly shifts away from the equllibrium site [1, 2, 3]. U_b^l is plotted as a function of domain thickness for three different values of E in Fig. 3(b). It is evident that the thickness sensitivity of U_b^l is more for higher values of E and U_b^l saturates at around the same thickness of Ω. As the magnitude of U_b^l reflects the contribution of far field region to the lattice resistance to a moving dislocation, we can expect a reduction in the dislocation velocity with increase in the domain thickness. We carry out MD simulations in order to verify this expectation.

The MD simulation procedures are similar to those described in our previous Letter [9]. We create freestanding thin films of bcc metals in the simulation cells of x and z dimensions as $39.5a<111>/2$ and $5a<1\bar{2}1>$ respectively, where a is the lattice constant. The y dimension along $<\bar{1}01>$ is varied to alter the film thickness. An edge dislocation is introduced at the middle of the cell with its line along the z axis and the Burgers vector $a<111>/2$ along the x direction. The cell boundaries are extended along the y direction to create free surfaces. Finnis-Sinclair interatomic potential model [13] is used with the parameters corresponding to Tungsten (W), Molybdenum (Mo) and Tantalum (Ta). Traction forces are applied to the top and bottom surfaces of the films to develop a shear stress of 250 MPa at a fixed temperature of 300 K, maintained using the Nosé-Hoover thermostat [14, 15]. Simulation proceeds in time steps of 0.5 fs and the dislocation position is recorded every 500 time steps so that the dislocation velocity can be extracted [16].

The dislocation velocities are plotted as a function of film thickness for W, Mo and Ta in Fig. 4. Although, these metals are anisotropic and the precise form of the singularity

distribution of the strain field due to a dislocation is unknown, we can still compare the trends of the plots between Fig. 4 and Fig. 3(b). Despite expressing the domain thickness in Fig. 3(b) in the units of the Burgers vector, we produce the exact plots in Fig. 4 without scaling as the lengths of the Burgers vectors of these metals are very close to one another (W:0.2741 nm, Mo:0.2725 nm, Ta:0.2862 nm). A drop in the dislocation velocity, followed by saturation at nearly the same film thickness (∼70-80 nm) for the three different metals (refer Fig. 4) is in accordance with the variation of U_b^l in Fig. 3(b). At this point, the MD results can be appreciated for serving a twofold purpose. Firstly, it reveals that the region significant for the lattice resistance is extended upto a few tens of nanometers from the dislocation line, which is much wider than the conventional estimates. Secondly, it shows that the size effect must be carefully included while analyzing the mechanical properties of the nanodimensional structures. During the prominant variation in the dislocation velocities, the thickness sensitivities can be determined from the slopes of the straight lines, fitted to the velocity data as shown in Fig. 4. These thickness sensitivites are tabulated against the elastic constants for the studied metals in Table-I. It worths pointing out that the thickness sensitivity follows the trend W>Mo>Ta and all the three elastic constants C_{11}, C_{12} and C_{44} [17] of these metals posses the same order as well. This again finds resemblance with the trend of U_b^l as obtained in Fig. 3(b). Thus, we find that the MD simulations provide conclusive results to prove the dependence of the lattice resistance on the elastic constants in the context of the contribution of the linear elastic region.

TABLE I: Elastic constants and thickness sensitivities

Metal	$C_{11}(GPa)$	$C_{12}(GPa)$	$C_{44}(GPa)$	$-\Delta v/\Delta y(\times 10^9 s^{-1})$
W	522.4	204.4	160.6	7.7
Mo	464.7	161.5	108.9	6.5
Ta	266.0	161.2	82.4	2.2

In a nutshell, we highlight a new theoretical standpoint that explains the origin of the lattice resistance by modelling a moving dislocation as a distributed singularity of the elastic field. It exhibits the existence of periodically occuring potential barrier to dislocation motion. The numerical findings of this model are in qualitative agreement with the results of the MD simulations. So far, we have demonstrated this through the calculations performed for

the far field region only. Nevertheless, the basic idea of strain field perturbation due to the singularity distribution is valid for the dislocation core too, at least at the conceptual level. In addition, the determination of more realistic forms of singularity distribution becomes an important aspect, whenever the exact quantificaion is required. Obviously, any attempt in this regard will suppliment the present work and contribute to develop a comprehensive theory of the lattice resistance.

MD++[18] molecular dynamics package has been used for the MD simulations in this work.

---

[1] R. E. Peierls, Proc. Phys. Soc. **52**, 23 (1940).

[2] F. R. N. Nabarro, Proc. Phys. Soc. **59**, 256 (1947).

[3] J. P. Hirth and J. Lothe, *Theory of Dislocations* (John Wiley and Sons., New York, 1982).

[4] Jian N. Wang, Acta Mater. **44**, 1541 (1996).

[5] B. Joós and M. S. Duesbery, Phys. Rev. Lett. **78**, 266 (1997).

[6] V. V. Bulatov and E. Kaxiras, Phys. Rev. Lett. **78**, 4221 (1997).

[7] G. Lu, N. Kioussis, V. V. Bulatov and E. Kaxiras, Phil. Mag. Lett. **80**, 675 (2000).

[8] W. Cai, V. V. Bulatov, J. Chang, J. Li and S. Yip, in *Dislocations in Solids*, edited by F. R. N. Nabarro and J. P. Hirth (North-Holland, New York, 2004), Chap 64.

[9] A. Dutta, M. Bhattacharya, P. Barat, P. Mukherjee, N. Gayathri and G. C. Das, Phys. Rev. Lett. **101**, 115506 (2008).

[10] G. Green, *In Mathematical papers of George Green*, edited by N. M. Ferrers (Chelsea, New York, 1999).

[11] M. Rahman, Proc. R. Soc. Lond. A **456**, 2021 (2000).

[12] W. P. Graebel, *Advanced Fluid mechanics*, (Academic Press, London, 2007)

[13] M. W. Finnis and J. E. Sinclair, Phil. Mag. **50**, 45 (1984).

[14] S. Nosé, Mol. Phys. **52**, 255 (1984).

[15] W. G. Hoover, Phys. Rev. A **31**, 1695 (1985).

[16] V. V. Bulatov and W. Cai, *Computer Simulations of Dislocations* (Oxford University Press, Oxford, 2006).

[17] The elastic constants are obtained by using the corresponding Finnis-Sinclair potential models [13] for W, Mo and Ta.

[18] http://micro.stanford.edu/

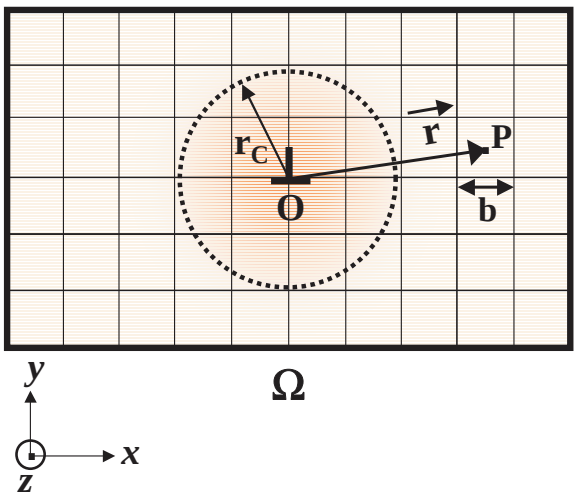

FIG. 1: (color online). Schematic representation of the computation method. Ω is the rectangular domain with an edge dislocation at the origin O. A typical square subdomain is shown with the position vector **r** from the origin to the centre of the subdomain. Calculations are done using such 200 subdomains along the x-direction on both sides of O. The number of subdomains along the y-direction is varied. The cut-off radius r_c represents the core region.

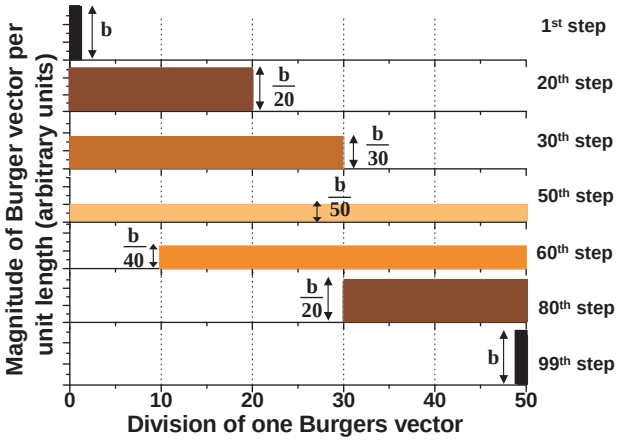

FIG. 2: (color online). (a) Schematic representation of the homogeneous distribution of the singularity of the strain field of an edge dislocation in discrete steps. Steps 1 to 50 show the extension of singularity up to the maximum delocalization, when the dislocation can be considered to be *halfway* between the two adjacent equilibrium sites. For the next half, the distribution contracts again to the line singularity in steps 51 to 99. After one full cycle, the dislocation shifts by one Burgers vector.

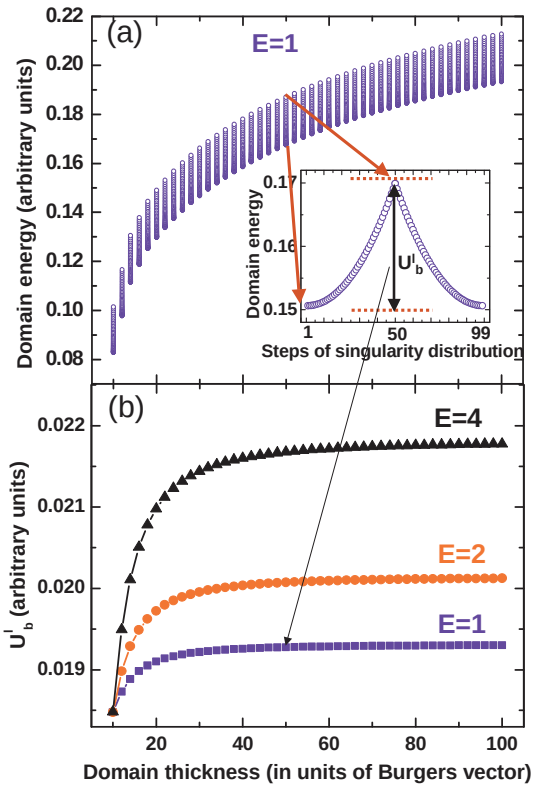

FIG. 3: (color online). (a) Variation of domain energy in discrete steps of singularity distribution is plotted as a function of domain thickness. The inset shows the existence of the potential energy barrier U_b^l for a particular domain size. (b) U_b^l is shown for three different Young's moduli, with the variation in the domain thickness. Suitable offsets are given to the data corresponding to E=2 and E=4 so that the initial data points of all the three curves coincide for an easier visual comparison of the slopes of these curves.

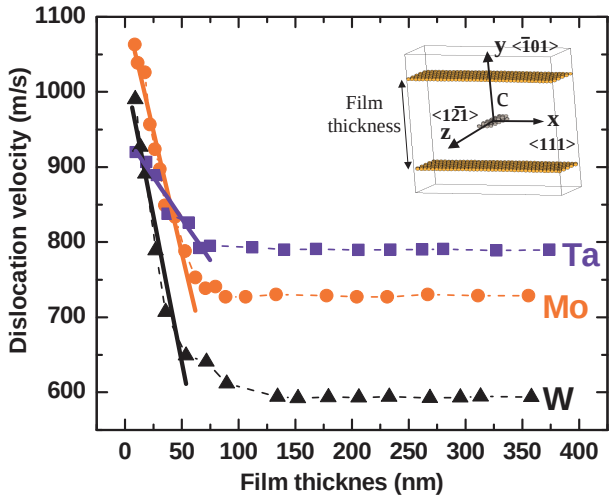

FIG. 4: (color online). Dislocation velocities obtained from MD simulations are presented as a function of film thickness for W (triangle), Mo (circle) and Ta (square). Fitted straight lines are shown for the velocities of all the three curves before saturation. A typical simulation cell with the indicated crystal directions and the dislocation core C is also displayed on the top-right corner.